



HAL
open science

Influence of NaX (X=I or Cl) additions on GeS₂-Ga₂S₃ based glasses

Antoine Brehault, Solenn Cozic, Rémi Boidin, Laurent Calvez, Eugène Bychkov, Pascal Masselin, Xianghua Zhang, David Le Coq

► **To cite this version:**

Antoine Brehault, Solenn Cozic, Rémi Boidin, Laurent Calvez, Eugène Bychkov, et al.. Influence of NaX (X=I or Cl) additions on GeS₂-Ga₂S₃ based glasses. *Journal of Solid State Chemistry*, 2014, 220, pp.238-244. 10.1016/j.jssc.2014.09.005 . hal-01069227

HAL Id: hal-01069227

<https://hal.science/hal-01069227>

Submitted on 9 Dec 2014

HAL is a multi-disciplinary open access archive for the deposit and dissemination of scientific research documents, whether they are published or not. The documents may come from teaching and research institutions in France or abroad, or from public or private research centers.

L'archive ouverte pluridisciplinaire **HAL**, est destinée au dépôt et à la diffusion de documents scientifiques de niveau recherche, publiés ou non, émanant des établissements d'enseignement et de recherche français ou étrangers, des laboratoires publics ou privés.



ELSEVIER

Contents lists available at ScienceDirect

Journal of Solid State Chemistry

journal homepage: www.elsevier.com/locate/jsscInfluence of NaX (X=I or Cl) additions on GeS₂–Ga₂S₃ based glassesA. Bréhault^a, S. Cozic^a, R. Boidin^b, L. Calvez^a, E. Bychkov^b, P. Masselin^b, X. Zhang^a,
D. Le Coq^{a,*}^a Institut des Sciences Chimiques de Rennes, Eq. Verres et Céramiques, UMR 6226 CNRS, Université de Rennes 1, 35042 Rennes Cedex, France^b Laboratoire de Physico Chimie de l'Atmosphère, EA 4493, Université du Littoral Côte d'Opale, 59140 Dunkerque, France

ARTICLE INFO

Article history:

Received 17 April 2014

Received in revised form

2 September 2014

Accepted 6 September 2014

Available online 16 September 2014

Keywords:

Chalcogenide glasses

Optical properties

Electrical conductivity

ABSTRACT

Chalcogenide glasses in the pseudo-ternary system NaX–GeS₂–Ga₂S₃ (X=Cl or I) were synthesized. Different series were investigated in order to highlight the influence of the sodium halide addition on two different host glasses (GeS₂)₈₀(Ga₂S₃)₂₀ and (GeS₂)₇₂(Ga₂S₃)₂₈. Macroscopic properties including density and characteristic temperatures, such as glass transition temperatures T_g and crystallization temperature T_x , were determined for a maximum molar content of NaX equal to 15%. The evolution of the optical band-gap and the chemical stability following the composition were also studied. Conductivity measurements were also performed and compared to other Li-based GeS₂–Ga₂S₃ glasses. The results were discussed taking into account the cation and anion nature and also the glass packing density.

© 2014 Elsevier Inc. All rights reserved.

1. Introduction

Chalcogenide glasses based on the GeS₂–Ga₂S₃ system are very attractive materials since they have low phonon energy, high refractive index and wide transmission range making them very good candidates in various fields. The structure of these pseudo-binary glasses has been widely investigated and literature proposes corner- and edge-shared Ge(Ga)S₄ tetrahedra, ethane-like S₃Ga–GaS₃ units connected by bridging sulfur, and more recently [Ge(Ga)S_{1/3}S_{3/p}]₃, (p=2, 3) triclusters [1–3]. Even this pseudo-binary system is already interesting thanks to its intrinsic properties, it is more pleasing because of the large possibility to be doped for optical or conductivity applications. For example, they possess a high solubility of rare-earth ions and consequently they are very promising as host glass matrix in the fluorescence material domain in the near- and mid-infrared regions [4–7]. Also, the possibility to add alkali halide in this system to extend the visible and infrared transparency range and to affect crystallization behavior by self-nucleating and nucleating agent was also used to promote phase separation and bulk nucleation [8,9]. Subsequently, reproducible infrared transmitting glass–ceramics with enhanced thermo-mechanical properties were produced [10,11]. The addition of alkali halide (MX) in germanium gallium sulfide glasses is also very suitable to obtain drastic increase of their ionic conductivity [12]. Indeed, chalcogenide glasses have better

potential than the oxide glasses for solid electrolyte applications [13,14]. Moreover, it has also been proved that partial crystallization can be profitable to enhance the ionic conductivity of the oxide or chalcogenide glasses [15,16].

Actually, the main reported works on the conductivity of MX–GeS₂–Ga₂S₃ glasses concern MX with M=Li⁺ or Ag⁺ and X=I[−] or Cl[−] [17,18]. Surprisingly, although the use of sodium salts (NaX) in the composition of chalcogenide glasses could be a good alternative as solid-state electrolyte in battery [19], the study of NaX-doped chalcogenide glass system is relatively poor.

This paper comes within the scope of preliminary study of sodium doped chalcogenide glasses in optic and conductivity fields. The influence of the included salt NaX (X=I[−] or Cl[−]) in two different host glass matrixes based on GeS₂ and Ga₂S₃ is investigated. Thus, the study of two different series for each of the two halogens will also assess the effect of the GeS₂/Ga₂S₃ ratio. Conductivity comparisons with ionic lithium doped GeS₂–Ga₂S₃ glasses are also done.

2. Experimental

2.1. Glass preparation

Glass sample compositions, (0.8GeS₂–0.2Ga₂S₃)_{100−x}(NaX)_x (X=Cl or I) and (0.72GeS₂–0.28Ga₂S₃)_{100−x}(NaX)_x (X=Cl or I) with 0 ≤ x ≤ 15, were synthesized from high purity elements (Ge, Ga, and S of 5 N) and compounds (NaI and NaCl of 2 N). Thereafter, the two host glass series 0.8GeS₂–0.2Ga₂S₃ and 0.72GeS₂–0.28Ga₂S₃

* Corresponding author. Tel.: +33 2 23 23 54 23; fax: +33 2 23 23 56 11.
E-mail address: david.lecoq@univ-rennes1.fr (D. Le Coq).

will further be $80\text{GeS}_2\text{-}20\text{Ga}_2\text{S}_3$ and $72\text{GeS}_2\text{-}28\text{Ga}_2\text{S}_3$, respectively. These components were weighed in glove box under Ar atmosphere in stoichiometric proportions and introduced in a silica ampoule. This ampoule was evacuated (10^{-5} Pa), sealed, and placed in a rocking furnace during 12 h at 850°C . The quench was operated in water at room temperature. The sample was finally annealed at $T_g - 30^\circ\text{C}$ for 4 h before being slowly cooled down to room temperature. The rod of 10 mm diameter was then cut into cylindrical or parallelepiped slices and after the polishing step the sample was approximately 1 mm thick. An analogous synthesis procedure with higher temperatures was carried out for lithium-based glasses.

2.2. Thermal and density analyses

The characteristic temperatures, glass transition temperature (T_g) and the crystallization temperature (T_x) corresponding to the onset points, of all these samples were determined with a differential scanning calorimeter (DSC Q20 Thermal Analysis). Glass samples were weighed and sealed in a hermetic aluminum pans. The experiments were performed from room temperature up to 550°C under nitrogen atmosphere using a heating rate of $10^\circ\text{C min}^{-1}$.

The measurement of sample density d was performed by a Archimedian method using distilled water as immersion fluid. A Mettler Toledo XS64 balance was used. The sample masses vary between 0.5 g and 1.5 g.

2.3. Optical measurements

Optical transmissions of these glasses were measured with a double beam spectrophotometer (Perkin Elmer Lambda 1050) in the visible and near IR ranges. The typical sample thickness was 1.00 mm (± 0.20 mm). The infrared transmission measurements were performed using a Bruker Vector 22 Spectrometer.

2.4. Impedance measurements

Total electrical conductivity of the samples showing a sufficient ionic conduction was measured with a Hewlett Packard 4194A impedance meter from room temperature to 473 K corresponding to a temperature below T_g for all the glass samples. The impedance measurements were carried out in a frequency range lying from 100 Hz to 15 MHz. For the other samples, we used a Hewlett

Packard 4339B high resistance meter with a 100V-applied voltage in order to determine the dc conductivity. The glass samples were prepared as discs of 10 mm diameter and 1 mm thickness with two parallel faces. The polished glass discs were then sputter coated with gold on both sides to form blocking electrodes, meaning that the electrochemical cell for conductivity measurements was Au/glass/Au. The temperature dependence on the conductivity was studied over several cycles. Each heating step measurement was followed by a cooling step measurement in order to study a possible hysteresis that was found to be negligible.

3. Results and discussion

3.1. Macroscopic properties

The characteristic temperatures T_g and T_x of investigated glass samples are given in Table 1. As shown in Fig. 1a, the decreasing evolution of T_g is systematic following the NaX content, whatever is the host glass. In the case of $(80\text{GeS}_2\text{-}20\text{Ga}_2\text{S}_3)_{100-x}(\text{NaX})_x$, $0 \leq x \leq 15$, T_g decreases from 442°C down to 370°C and 364°C for NaCl and NaI, respectively. For the other host glass, $(72\text{GeS}_2\text{-}28\text{Ga}_2\text{S}_3)_{100-x}(\text{NaX})_x$, $0 \leq x \leq 15$, the decrease is less pronounced since T_g decreases from 428°C down to 383°C and 382°C for NaCl and NaI, respectively. This behavior is not surprising since other works in $\text{GeS}_2\text{-Ga}_2\text{S}_3$ based systems have shown a similar trend, notably in the pseudo-ternary $\text{GeS}_2\text{-Ga}_2\text{S}_3\text{-CsCl}$ or CsI system [20,21]. This is traditionally ascribed to the progressive breaking of Ge-S or Ga-S bonds forming $\text{Ga}(\text{Ge})\text{S}_{3/2}\text{X}^-$ that leads to a decrease of the connectivity of the glass network. Fig. 1a also displays greater NaX dependence for the $80\text{GeS}_2\text{-}20\text{Ga}_2\text{S}_3$ series in comparison with the $72\text{GeS}_2\text{-}28\text{Ga}_2\text{S}_3$ one, meaning that a higher content of Ga_2S_3 in the host glass composition seems important to keep highest T_g .

The ΔT parameter, corresponding to the difference between T_g and T_x is important to evaluate the thermal stability of the glass. Here, whatever the composition, almost all ΔT becomes higher than 100°C meaning that glass samples are stable. Indeed, their evolution as a function of the NaX content is plotted in Fig. 1b and it is noticed that ΔT increases although T_g decreases. The more positive effect of NaI compared to NaCl is also observed since the slope of the ΔT evolution is superior from both host glasses. Besides ΔT , two other parameters based on the characteristic temperatures are regularly explored in order to characterize the glasses. The first one is the so-called Hruby criterion $H_r = (T_x - T_g)/(T_m - T_x)$, which is

Table 1

Values of selected parameters for the studied glasses including the glass transition temperature T_g , the crystallization temperature T_x , the density d , and the optical band gap E_g . Glass-forming and thermal stability criteria are also given: $\Delta T = T_x - T_g$ and a criterion for glass ability against crystallization $H' = \Delta T/T_g$.

Sample composition	T_g ($\pm 2^\circ\text{C}$)	T_x ($\pm 2^\circ\text{C}$)	ΔT ($\pm 4^\circ\text{C}$)	H' (± 0.008)	d (± 0.01 g cm $^{-3}$)	E_g (± 0.02 eV)
$80\text{GeS}_2\text{-}20\text{Ga}_2\text{S}_3$	442	520	78	0.109	2.93	2.64
$(80\text{GeS}_2\text{-}20\text{Ga}_2\text{S}_3)_{90}(\text{LiI})_{10}$	406	532	126	0.186	2.99	/
$(80\text{GeS}_2\text{-}20\text{Ga}_2\text{S}_3)_{95}(\text{NaCl})_5$	420	530	110	0.159	2.90	2.73
$(80\text{GeS}_2\text{-}20\text{Ga}_2\text{S}_3)_{90}(\text{NaCl})_{10}$	396	535	139	0.208	2.87	2.81
$(80\text{GeS}_2\text{-}20\text{Ga}_2\text{S}_3)_{85}(\text{NaCl})_{15}$	370	521	151	0.235	2.85	2.83
$(80\text{GeS}_2\text{-}20\text{Ga}_2\text{S}_3)_{95}(\text{NaI})_5$	418	536	118	0.171	2.96	2.63
$(80\text{GeS}_2\text{-}20\text{Ga}_2\text{S}_3)_{90}(\text{NaI})_{10}$	390	541	151	0.228	2.99	2.66
$(80\text{GeS}_2\text{-}20\text{Ga}_2\text{S}_3)_{85}(\text{NaI})_{15}$	364	531	177	0.278	3.02	2.69
$72\text{GeS}_2\text{-}28\text{Ga}_2\text{S}_3$	428	485	57	0.081	3.00	2.58
$(72\text{GeS}_2\text{-}28\text{Ga}_2\text{S}_3)_{90}(\text{LiI})_{10}$	382	498	116	0.177	3.04	/
$(72\text{GeS}_2\text{-}28\text{Ga}_2\text{S}_3)_{95}(\text{NaCl})_5$	410	490	80	0.117	2.96	2.66
$(72\text{GeS}_2\text{-}28\text{Ga}_2\text{S}_3)_{90}(\text{NaCl})_{10}$	394	503	109	0.163	2.92	2.74
$(72\text{GeS}_2\text{-}28\text{Ga}_2\text{S}_3)_{85}(\text{NaCl})_{15}$	383	519	136	0.207	2.89	2.85
$(72\text{GeS}_2\text{-}28\text{Ga}_2\text{S}_3)_{95}(\text{NaI})_5$	413	500	87	0.126	3.01	2.63
$(72\text{GeS}_2\text{-}28\text{Ga}_2\text{S}_3)_{90}(\text{NaI})_{10}$	401	530	129	0.191	3.03	2.68
$(72\text{GeS}_2\text{-}28\text{Ga}_2\text{S}_3)_{85}(\text{NaI})_{15}$	382	/	/	/	3.05	2.70

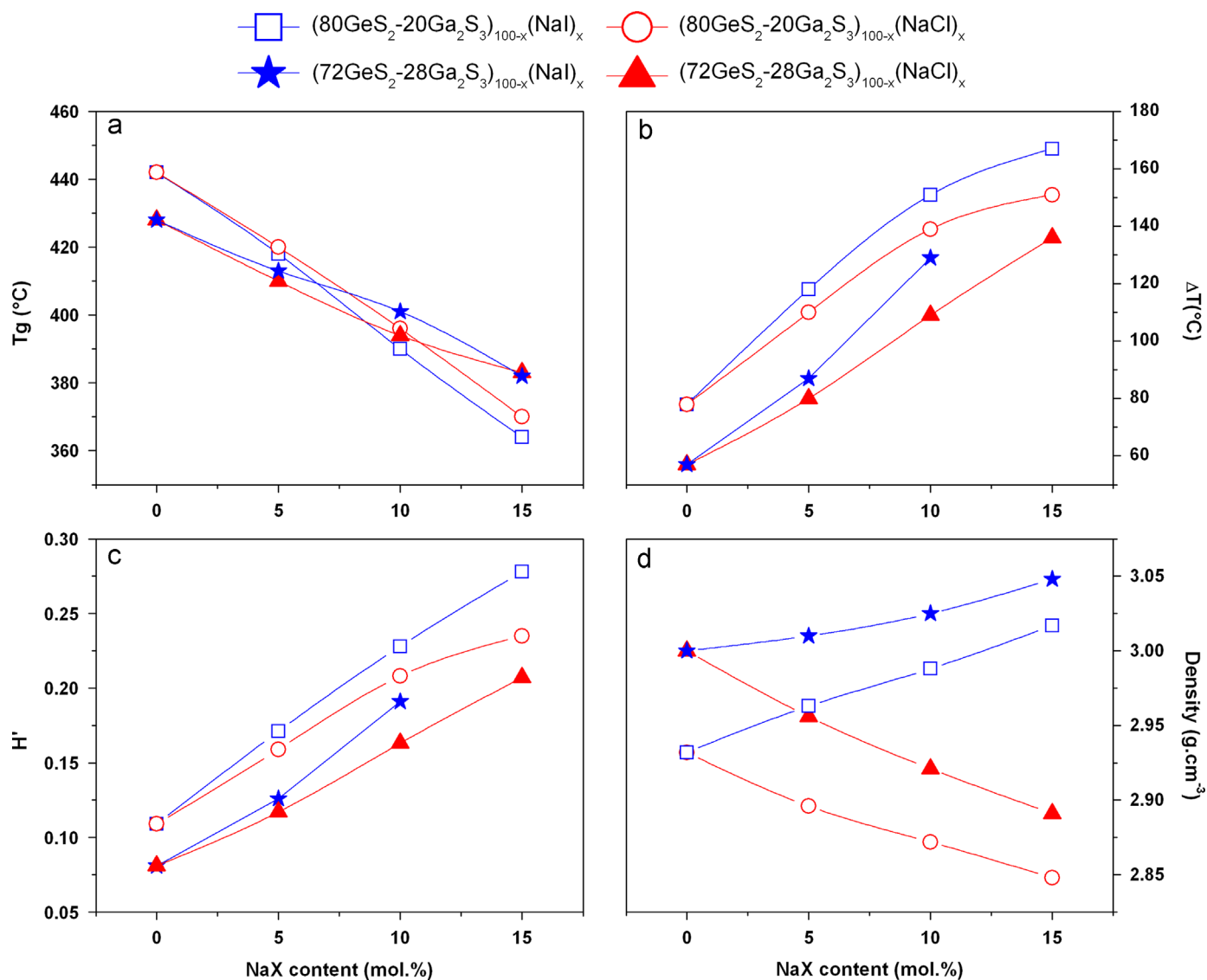


Fig. 1. Evolution of thermal and density parameters as a function of the NaX content x , $0 \leq x \leq 15$, with $X = \text{Cl}$ or I : (a) the glass transition temperature T_g , (b) the difference between T_g and T_x , ΔT , corresponding to the crystallization temperature, (c) the criterion H' relative to the stability of the glass against crystallization, and (d) the density.

used to evaluate the glass forming ability [22]. In case of high melting temperatures T_m , an alternative criterion H' is also used to estimate the glass forming ability against crystallization, $H' = \Delta T/T_g$ [23]. This last parameter, plotted in Fig. 1c, exhibits similar trend than the ΔT parameter following the NaX content. Finally, H' and ΔT values increase following the NaX additions meaning that both thermal stability and glass forming ability are better for the richest NaX-bearing compositions. This can be attributed to the halogenide anions X^- that are well known to progressively break the Ge–S or Ga–S bonds and partially form the complex anion $\text{Ga}(\text{Ge})\text{S}_{3/2}X^-$ tetrahedral. This structural unit is then assumed to favor the glass formation [24]. The results also point out the more positive effect of the iodide salt comparatively to the chloride one.

The evolution of the density exhibited in Fig. 1d is different for sodium chloride- and sodium iodide-bearing glasses. In NaCl-based glasses, the density monotonously decreases following the NaCl content whereas in NaI-based glasses it monotonously increases. These contrary behaviors can be ascribed to the relative mean atomic weights of NaCl and NaI compared to the host glass ones. For NaCl it is 29.2 g and for NaI it is 75.0 g, whereas for $80\text{GeS}_2-20\text{Ga}_2\text{S}_3$ and $72\text{GeS}_2-28\text{Ga}_2\text{S}_3$, the relative mean atomic weights are 45.8 g and 45.9 g, respectively.

3.2. Optical properties

The addition of NaX in GeS_2 – Ga_2S_3 based glasses is characterized by a blue-shift of the visible transmission as shown in Fig. 2a for the selected compositions $(72\text{GeS}_2-28\text{Ga}_2\text{S}_3)_{100-x}(\text{NaX})_x$, with $X = \text{I}$ or Cl and $5 \leq x \leq 15$. A photograph of two different glasses after polishing are also given; the parallelepiped and tablet samples correspond to the composition $(72\text{GeS}_2-28\text{Ga}_2\text{S}_3)_{90}(\text{NaI})_{10}$ and $(72\text{GeS}_2-28\text{Ga}_2\text{S}_3)_{90}(\text{NaCl})_{10}$, respectively. In Fig. 2b, the evolution of the optical band gap E_g for the four investigated series are plotted. As first observation, we can notice that E_g grows up whatever the sodium halogenide added in the host glass. The second observation is the lower increase of E_g when the sodium iodide is added instead of the sodium chloride. From the $(80\text{GeS}_2-20\text{Ga}_2\text{S}_3)$ host glass E_g evolves from 0.05 eV and 0.19 eV by adding up to 15 mol% of NaI and NaCl, respectively, and from the $(72\text{GeS}_2-28\text{Ga}_2\text{S}_3)$ host glass E_g progresses from 0.12 eV and 0.27 eV in similar conditions. These general behaviors are often observed when halogen is introduced in the composition of a chalcogenide glasses [20]. As already mentioned, the introduction of chlorine or iodine is supposed to progressively break the Ge–S or Ga–S to form $\text{Ga}(\text{Ge})\text{S}_{4-y}X_y$ tetrahedral units. In other words, the average number

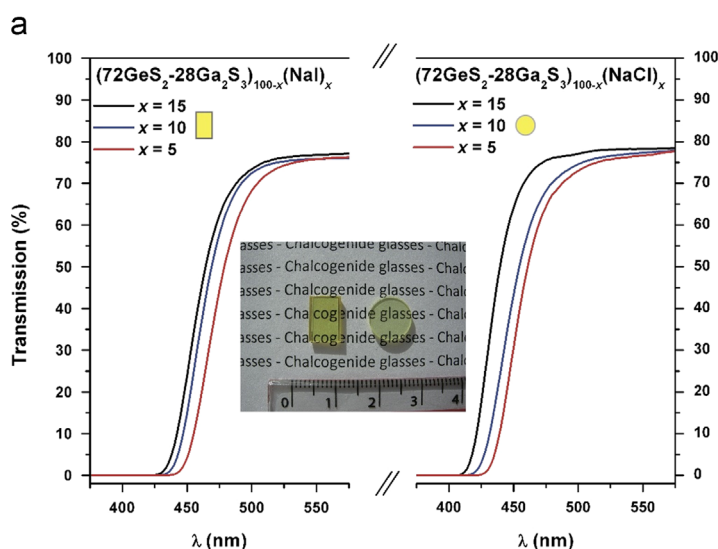


Fig. 2. (a) Visible transmission spectra of $(72\text{GeS}_2-28\text{Ga}_2\text{S}_3)_{100-x}(\text{NaX})_x$ glasses, with $X=\text{I}$ or Cl and $5 \leq x \leq 15$. The photograph is focusing on the parallelepiped and tablet glass samples corresponding to the specific composition $(72\text{GeS}_2-28\text{Ga}_2\text{S}_3)_{90}(\text{NaI})_{10}$ and $(72\text{GeS}_2-28\text{Ga}_2\text{S}_3)_{90}(\text{NaCl})_{10}$, respectively. (b) Evolution of the optical band gap of the four series $(72\text{GeS}_2-28\text{Ga}_2\text{S}_3)_{100-x}(\text{NaX})_x$ and $(80\text{GeS}_2-20\text{Ga}_2\text{S}_3)_{100-x}(\text{NaX})_x$ glasses, with $X=\text{I}$ or Cl and $5 \leq x \leq 15$.

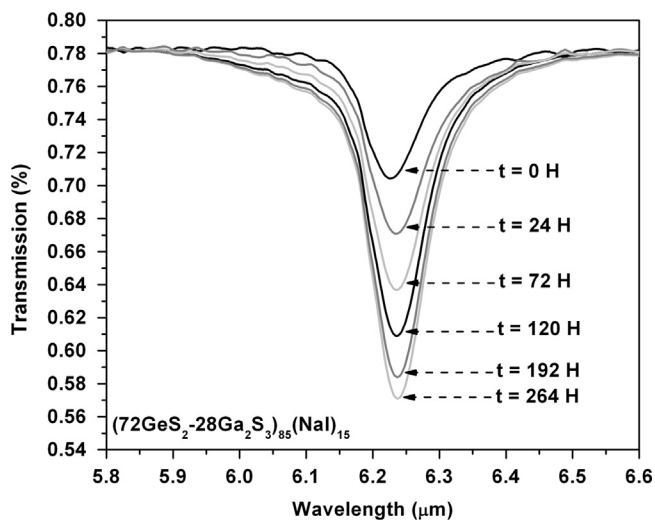


Fig. 3. Evolution of the H_2O absorption band located at $6.23 \mu\text{m}$ after different time ($t=0 \text{ h}$, 24 h , 72 h , 120 h , 192 h , and 264 h) for the specific composition $(72\text{GeS}_2-28\text{Ga}_2\text{S}_3)_{85}(\text{NaI})_{15}$.

of Ge–S and Ga–S bonds is lower and the Ge–Cl or Ge–I ones is increased. In Pauling scale, the electronegativity of Ga, Ge, S, Cl, and I are 1.81, 2.01, 2.58, 3.16, and 2.66, respectively. So, the electronegativity difference of the Ga–S is 0.77 and Ge–S is 0.57 whereas for Ga–Cl it is 1.35, Ge–Cl it is 1.15, Ga–I it is 0.85, and Ge–I it is 0.65. Consequently, the average electronegativity of the material grows up if Cl^- or I^- anions are added in the composition of the glasses leading to a low wavelength-shift of E_g [25]. This explanation is supported by the lower white-shift of the NaI based samples comparatively to the NaCl ones.

3.3. Resistance to humidity

Alkali halide compounds are well known to be poorly resistant towards humidity. To evaluate the effect of the progressive addition of NaX in the host glasses it is possible to observe the evolution of the water absorption band located around $6.23 \mu\text{m}$ as the function of the time. The first infrared transmission measurement was implemented just after polishing in ethanol.

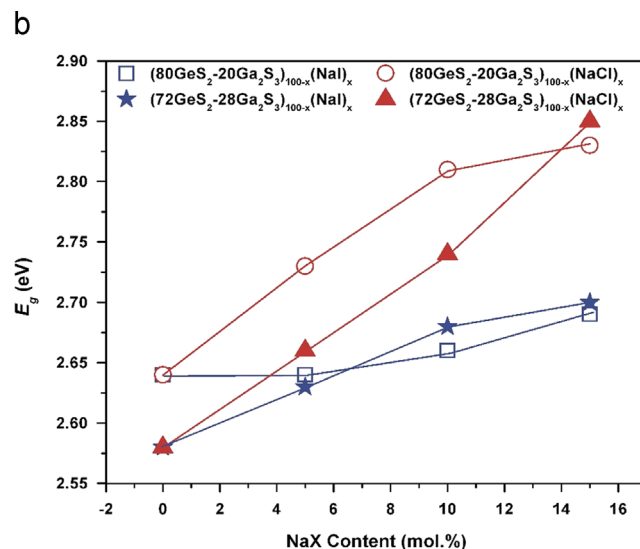


Fig. 3 emphasizes its increasing evolution for the particular glass sample $(72\text{GeS}_2-28\text{Ga}_2\text{S}_3)_{85}(\text{NaI})_{15}$ after 0 h, 24 h, 72 h, 120 h, 192 h, and 264 h without any additional polishing. Analogous study was carried out for other glasses ($(72\text{GeS}_2-28\text{Ga}_2\text{S}_3)_{100-x}(\text{NaX})_x$ glasses, with $X=\text{I}$ or Cl and $5 \leq x \leq 15$) and **Fig. 4** exhibits the evolution of their H_2O band intensity. It is clearly observed that the increasing intensity is more pronounced in the case of NaI based glasses. No surprisingly, as observed in **Fig. 4**, this growing evolution is more important for the high content in NaX. One can also observe that the intensity is growing up for all samples and that this increase is more important in the first hours. This is consistent with a corrosion of the samples majority, indeed exclusively, at their surfaces, already observed for other chalcogenide glasses in more drastic conditions [26]. The corrosion mechanism is probably due to the ion exchange between halide ions and hydroxyl ions OH^- that occurs at the glass surface. Since iodine is less electronegative than chlorine the substitution between I^- and OH^- anions is easier than between Cl^- and OH^- anions at the glass surface, meaning that the stability against humidity is less in case of NaI-bearing glasses compared to NaCl-bearing glasses.

3.4. Electrical conductivity

Complex impedance plots of the $(80\text{GeS}_2-20\text{Ga}_2\text{S}_3)_{90}(\text{NaCl})_{10}$ glasses at different temperatures is shown in **Fig. 5a** as typical example. In **Fig. 5b**, other plots recorded at 100°C are shown. They correspond to glass samples containing 10 mol% of NaCl or LiI in $80\text{GeS}_2-20\text{Ga}_2\text{S}_3$ or $72\text{GeS}_2-28\text{Ga}_2\text{S}_3$. **Fig. 5a** exhibits an expected trend as a function of the temperature. Whatever the temperature, we can observe the typical spectrum of an ionic conductor, which consisted in a high-frequency semi-circle and a low-frequency tail. This low-frequency polarization characterizes the difficulties of the charge transfer at the Au/Glass interface of the electrochemical cell. This phenomenon seems to be more pronounced for Li-based glasses compared to the Na-based ones.

The linear temperature dependence on the conductivity σ for selected glasses is exhibited in **Fig. 6**. All data obey the Arrhenius law

$$\sigma = \frac{\sigma_0}{T} \exp\left(\frac{-E_\sigma}{kT}\right) \quad (1)$$

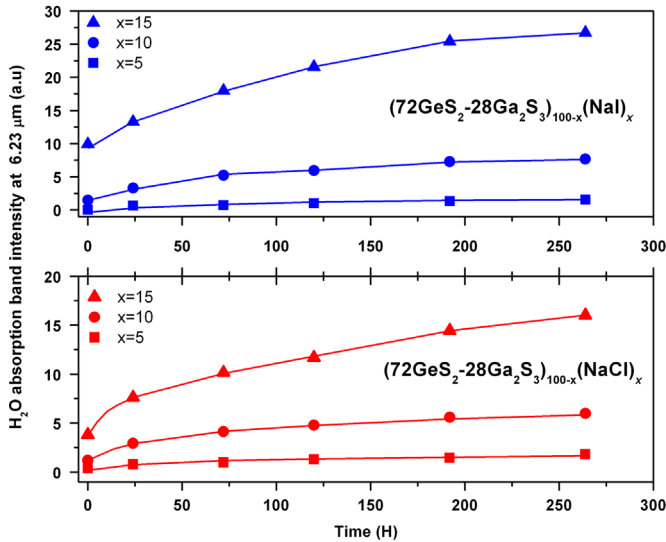


Fig. 4. Evolution of the H_2O absorption band intensity located at $6.23 \mu\text{m}$ after different time ($t=0$ h, 24 h, 72 h, 120 h, 192 h, 264 h) for $(72\text{GeS}_2-28\text{Ga}_2\text{S}_3)_{100-x}-(\text{NaX})_x$ glasses, with $X=\text{I}$ or Cl and $5 \leq x \leq 15$.

where σ_0 is the pre-exponential factor, E_a is the activation energy, k is the Boltzmann constant and T is the temperature. E_a , σ_0 , and the room-temperature conductivity σ_{298} were obtained by fitting the conductivity to the Arrhenius equation and are listed in Table 2.

The investigated glasses over the limited composition range show a few changes in the room-temperature conductivity σ_{298} . The σ_{298} increases with mobile cation concentration from $3.9 \times 10^{-8} \text{ S cm}^{-1}$ (NaI-doped glass, 2.9 at% Na) to $1.8 \times 10^{-6} \text{ S cm}^{-1}$ ($\text{Li}_2\text{S}-\text{Ga}_2\text{S}_3-\text{GeS}_2$, 5.7 at% Li) while the mobile cation content is doubled (Fig. 7). The conductivity activation energy varies weakly between 0.53 and 0.58 eV. Our results agree reasonably well with the published conductivity data on similar glassy systems [16,24,27]

As expected, Li^+ ion conducting glasses show a better ionic transport at comparable cation concentration x of ≈ 3 at%. Nevertheless, at higher x both Li^+ and Na^+ glassy systems seem to have similar conductivity parameters. We did not observe either a pronounced positive effect of large polarizable iodine anion on the ionic transport properties in the $\text{MX}-\text{Ga}_2\text{S}_3-\text{GeS}_2$ glasses over the investigated composition range in marked contrast to other chalcogenide glassy systems [28–30]. In addition, the lithium sulfide vitreous alloy also shows a higher conductivity at 298 K compared to LiCl-, LiI-, NaCl- and NaI-containing glasses (Fig. 7). The influence of the glass matrix composition, in other words, the $\text{GeS}_2/\text{Ga}_2\text{S}_3$ ratio is found to be weakly significant compared to the effect of the cation. Indeed, for the three investigated salt MX (NaI, NaCl, and LiI) one can see a higher conductivity for the 80/20 ratio comparatively to the 72/28 ratio. This observation is consistent with a future study in which this trend is confirmed by investigating other $\text{GeS}_2/\text{Ga}_2\text{S}_3$ ratios [31].

In order to solve the observed puzzle, further conductivity measurements over extended composition range are needed and especially the advanced structural studies. However, in current situation, we can ask whether the relative insensitivity of the glass ionic conductivity to the chemical form of ionic dopant (MI, MCl or M_2S) is related to the glass packing density ρ [32,33]. This empiric structural parameter is a ratio between the average atomic volume of the glass constituents V_a^0 , calculated using glass stoichiometry and ionic radii, and the average glass atomic volume V_a derived from glass stoichiometry and density

$$\rho = \frac{V_a^0}{V_a} \quad (2)$$

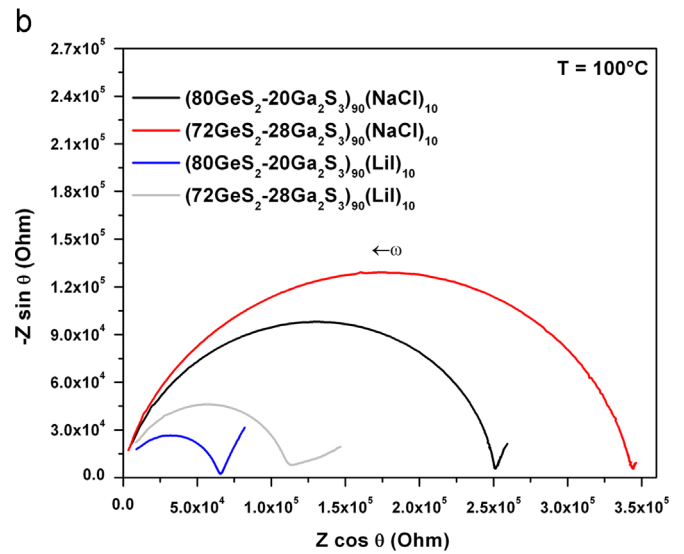
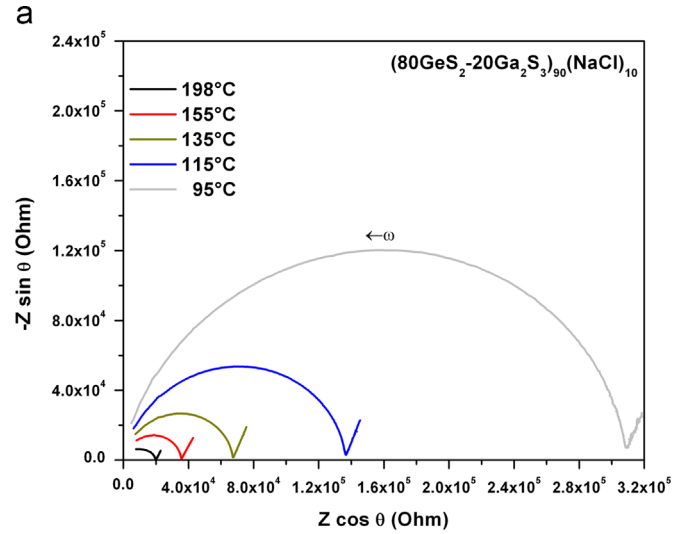


Fig. 5. (a) Evolution of the Cole-Cole diagrams of the specific glass composition $(80\text{GeS}_2-20\text{Ga}_2\text{S}_3)_{90}(\text{NaCl})_{10}$ for different temperatures T . (b) Isothermal (100°C) Cole-Cole diagrams for different glass compositions.

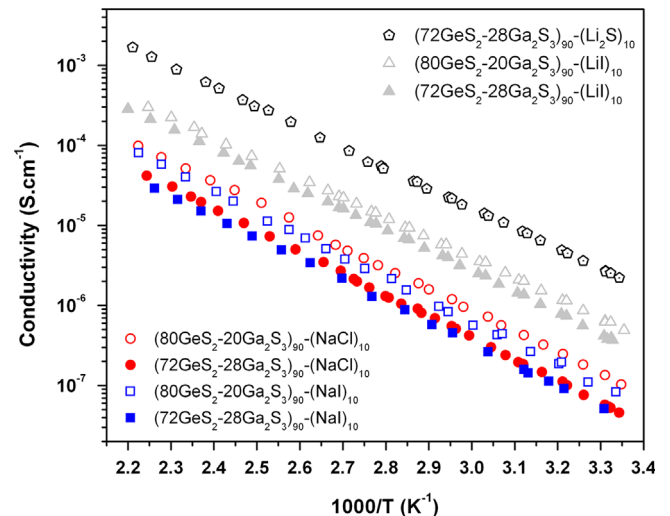


Fig. 6. Temperature dependence of the total electrical conductivity σ for glass compositions containing 10 mol% of NaCl, NaI, LiI, and Li_2S in $80\text{GeS}_2-20\text{Ga}_2\text{S}_3$ (open symbols) or $72\text{GeS}_2-28\text{Ga}_2\text{S}_3$ (full symbols).

Table 2

Conductivity parameters for selected glass compositions: the room-temperature conductivity σ_{298} , the activation energy E_a and the pre-exponential factor σ_0 . Uncertainties on the last digit are given in parentheses.

Composition	$\log \sigma_{298}$ (S cm ⁻¹)	E_a (eV)	$\log \sigma_0$ (S cm ⁻¹ K)
(80GeS ₂ -20Ga ₂ S ₃) ₉₀ -(LiI) ₁₀	-6.34 (5)	0.535 (4)	5.18 (5)
(80GeS ₂ -20Ga ₂ S ₃) ₉₀ -(NaCl) ₁₀	-6.92 (5)	0.544 (4)	4.75 (5)
(80GeS ₂ -20Ga ₂ S ₃) ₉₀ -(NaI) ₁₀	-7.24 (3)	0.582 (3)	5.08 (3)
(72GeS ₂ -28Ga ₂ S ₃) ₉₀ -(Li ₂ S) ₁₀	-5.74 (3)	0.545 (3)	5.95 (3)
(72GeS ₂ -28Ga ₂ S ₃) ₉₀ -(LiI) ₁₀	-6.44 (2)	0.529 (2)	4.97 (2)
(72GeS ₂ -28Ga ₂ S ₃) ₉₀ -(NaCl) ₁₀	-7.34 (4)	0.561 (4)	4.62 (4)
(72GeS ₂ -28Ga ₂ S ₃) ₉₀ -(NaI) ₁₀	-7.41 (3)	0.554 (2)	4.43 (5)

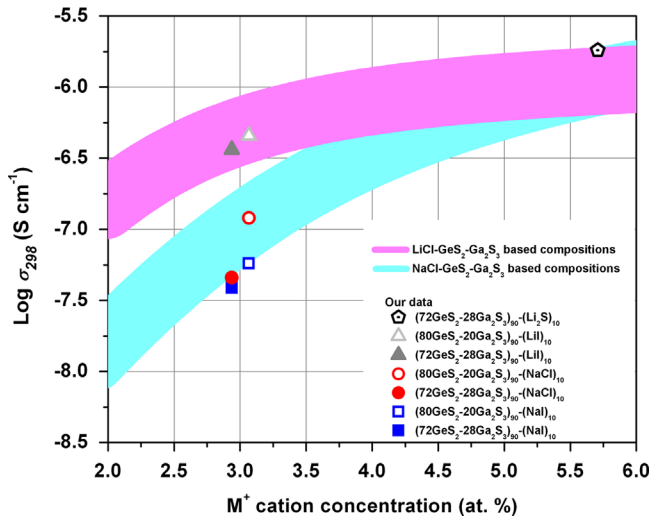


Fig. 7. Room-temperature conductivity σ_{298} of investigated glasses: (i) (80GeS₂-20Ga₂S₃)₉₀(MX)₁₀ (open symbols) with MX=NaI (blue) or NaCl (red) or LiI (light gray), (ii) (72GeS₂-28Ga₂S₃)₉₀(MX)₁₀ (full symbols) with MX=NaI (blue) or NaCl (red) or LiI (light gray), and (iii) (72GeS₂-28Ga₂S₃)₉₀(Li₂S)₁₀ (black symbol). The reported data corresponding to mean conductivity at 298 K [23,26] for the NaCl-Ga₂S₃-GeS₂ (blue line) and LiCl-Ga₂S₃-GeS₂ (light brown line) glassy systems are also shown for comparison. (For interpretation of the references to color in this figure legend, the reader is referred to the web version of this article.)

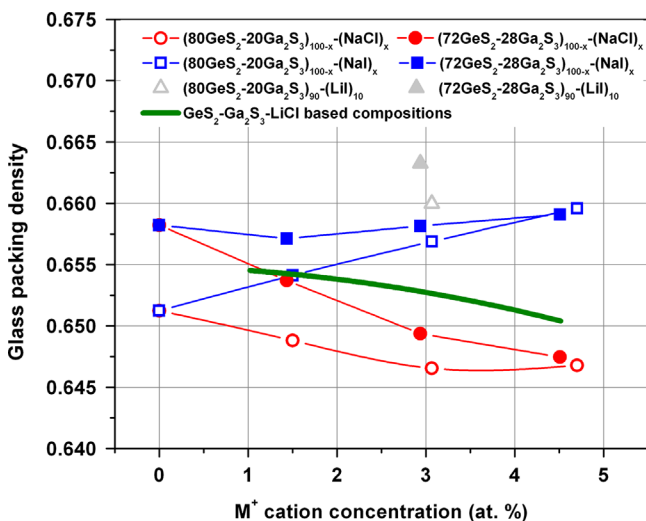


Fig. 8. The derived glass packing density ρ of the investigated glasses as a function of the M⁺ cationic concentration: (i) (80GeS₂-20Ga₂S₃)_{100-x}(MX)_x (open symbols) with MX=NaCl (red) or NaI (blue) or LiI (light gray), (ii) (72GeS₂-28Ga₂S₃)_{100-x}(MX)_x (full symbols) with MX=NaCl (red) or NaI (blue) or LiI (light gray). The reported glass packing density ρ [26] for the LiCl-Ga₂S₃-GeS₂ (green line) is also shown for comparison. (For interpretation of the references to color in this figure legend, the reader is referred to the web version of this article.)

$$V_a^0 = \sum_i c_i \frac{4\pi}{3} r_i^3 \quad (3)$$

$$V_a = \frac{\sum_i c_i M_i}{d N_A} \quad (4)$$

where c_i is the atomic fraction of the element i , M_i and r_i are the respective atomic mass and Shannon ionic radius, N_A the Avogadro constant. The high glass packing density $\rho \rightarrow 1$ means the absence of free space for atomic motion similar to negative effect of high-pressure on the ionic transport [34,35]. The opposite case, low ρ , is favorable for fast ionic mobility. Large cationic (Pb, Hg, etc.) and anionic (I, Te, etc.) species are suggested to increase the ionic conductivity via the increasing available free volume [36,37]. The calculated glass packing densities for the investigated glasses are shown in Fig. 8. Surprisingly, neither lithium nor sodium iodides do significantly increase the available free volume ($1-\rho$) in the glass, thus explaining the relative insensitivity of the chemical doping form (MCl vs. MI) on the Li⁺ or Na⁺ ionic conductivity in the MX-Ga₂S₃-GeS₂ glasses over limited composition range.

4. Conclusion

Glass samples in the NaX-GeS₂-Ga₂S₃ system, with X=Cl or I have been prepared. Whatever is the halide, the increment of the NaX molar percentage leads to a similar trend for thermal characteristics. A decrease of the glass transition temperature and an increase of both glass-forming ability and thermal stability have been emphasized. At contrary, density shows reverse behaviors, which has been attributed to the mass of the sodium halide. The temperature dependence of the conductivity, which has to be considered as ionic, follows an Arrhenius type equation for all investigated glasses. The relative low effect of the chemical doping form (MCl vs. MI) on the ionic conductivity coming from the mobility of the Na⁺ or Li⁺ cations has been discussed following a hypothesis based on the glass packing density.

Acknowledgments

This work is funded by the ‘‘Agence Nationale de la Recherche’’ through the ASTRID program and the ‘‘Direction G n rale de l’Armement’’.

References

- [1] H. Guo, Y. Zhai, H. Tao, G. Dong, X. Zhao, Mater. Sci. Eng. B Solid 138 (2007) 235–240.
- [2] A. Tverjanovich, Y.S. Tveryanovich, S. Loheider, J. Non-Cryst. Solids 208 (1996) 49–55.
- [3] P. Masselin, D. Le Coq, A. Cuisset, E. Bychkov, Opt. Mater. Exp. 2 (12) (2012) 1768–1775.
- [4] K. Wei, D.P. Machewirth, J. Wenzel, E. Snitzer, G.H. Sigel, J. Non-Cryst. Solids 182 (1995) 257–261.
- [5] A. Tverjanovich, Ya.G. Grigoriev, S.V. Degtyarev, A.V. Kurochkin, A.A. Man'shina, Yu.S. Tver'yanovich, J. Non-Cryst. Solids 286 (2001) 89–92.
- [6] T.Yu. Ivanova, A.A. Man'shina, A.V. Kurochkin, Yu.S. Tver'yanovich, V.B. Smirnov, J. Non-Cryst. Solids 298 (2002) 7–14.
- [7] B. Fan, C. Point, J.-L. Adam, X. Zhang, X. Fan, H. Ma, J. Appl. Phys. 110 (11) (2011) 113107–113108.
- [8] H. Ma, L. Calvez, B. Bureau, M.L. Floch, X. Zhang, J. Lucas, J. Phys. Chem. Solids 68 (2007) 968–971.
- [9] L. Calvez, H. Ma, J. Lucas, P. Glouannec, X. Zhang, J. Non-Cryst. Solids 353 (2007) 4702–4706.
- [10] C. Lin, L. Calvez, H. Tao, M. Allix, A. Mor eac, X.H. Zhang, X. Zhao, J. Solids State Chem. 184 (3) (2011) 584–588.
- [11] Y. Ledemi, B. Bureau, L. Calvez, M. Le Floch, M. Roz e, C. Lin, X.H. Zhang, M. Allix, G. Matzen, Y. Messaddeq, J. Phys. Chem. B 113 (44) (2009) 14474–14580.
- [12] W. Yao, S.W. Martin, Solid State Ion. 178 (2008) 1777–1784.
- [13] M. Yamashita, H. Yamanaka, Solid State Ion. 158 (2003) 151–156.
- [14] J. Saienga, S.W. Martin, J. Non-Cryst. Solids 354 (2008) 1475–1486.

- [15] B. Roling, A. Schirmeisen, H. Bracht, A. Taskiran, H. Fuchs, S. Murugavel, F. Natrup, *Phys. Chem. Chem. Phys.* 7 (2005) 1472–1475.
- [16] C. Lin, L. Calvez, B. Bureau, T. Haizheng, M. Allix, Z. Hao, V. Seznec, X. Zhang, X. Zhao, *Phys. Chem. Chem. Phys.* 12 (2010) 3780–3787.
- [17] S. Stehlik, V. Zima, T. Wagner, J. Ren, M. Frumar, *Solid State Ion.* 179 (2008) 1867–1875.
- [18] J. Kolář, T. Wágner, V. Zima, Š. Stehlik, B. Frumarová, L. Beneš, M. Vlček, M. Frumar, S.O. Kasap, *J. Non-Cryst. Solids* 357 (11–13) (2011) 2223–2227.
- [19] A. Hayashi, K. Noi, A. Sakuda, M. Tatsumisago, *Nat. Commun.* 3 (2012) 856.
- [20] P. Masselin, D. Le Coq, L. Calvez, E. Petracovschi, E. Lépine, E. Bychkov, X.H. Zhang, *Appl. Phys. A Mater. Sci. Process.* 106 (3) (2012) 697–702.
- [21] C. Lin, G.S. Qu, Z.B. Li, S.X. Dai, H.L. Ma, T.F. Xu, Q.H. Nie, X.H. Zhang, *J. Am. Ceram. Soc.* 96 (6) (2013) 1779–1782.
- [22] A. Hruby, *Czech. J. Phys. B* 22 (1972) 1187–1193.
- [23] J. Heo, J.K. Park, Y.S. Kim, *J. Non-Cryst. Solids* 175 (2–3) (1994) 204–210.
- [24] Y.S. Tver'yanovich, V.V. Aleksandrov, I.V. Murin, E.G. Nedoshovenko, *J. Non-Cryst. Solids* 256–257 (1999) 237–241.
- [25] M.P. Hehlen, B.L. Bennett, A. Castro, D.J. Williams, S.C. Tornga, R.E. Muenchausen, *Opt. Mater.* 32 (2010) 491–499.
- [26] L. Calvez, P. Lucas, M. Rozé, H.L. Ma, J. Lucas, X.H. Zhang, *Appl. Phys. A* 89 (2007) 183–188.
- [27] Z.U. Borisova, E.A. Bychkov, Yu.S. Tver'yanovich, *Interaction of Metals with Chalcogenide Glasses*, Leningrad State University, Leningrad, 1991.
- [28] J.P. Malugani, G. Robert, *Mater. Res. Bull.* 14 (1979) 1075–1081.
- [29] B. Carette, M. Maurin, M. Ribes, M. Duclot, *Solid State Ion.* 9–10 (1983) 655–658.
- [30] E. Bychkov, D.L. Price, C.J. Benmore, A.C. Hannon, *Solid State Ion.* 154–155 (2002) 349–359.
- [31] A. Bréhault, S. Cozic, L. Calvez, X.H. Zhang, D. Le Coq, 2014, in preparation.
- [32] U. Hoppe, *J. Non-Cryst. Solids* 248 (1999) 11–18.
- [33] A. Masuno, S. Kohara, A.C. Hannon, E. Bychkov, H. Inoue, *Chem. Mater.* 25 (2013) 3056–3061.
- [34] S.W. Kurnick, *J. Chem. Phys.* 20 (1952) 218–228.
- [35] H. Mehrer, A.W. Imre, E. Tanguet-Nijokep, *J. Phys.: Conf. Ser.* 106 (2008) 012001.
- [36] Yu.G. Vlasov, E.A. Bychkov, B.L. Seleznev, *Solid State Ion.* 24 (1987) 179–187.
- [37] R. Boidin, I. Alekseev, K. Michel, D. Le Coq, E. Bychkov, *Solid State Ion.* 262 (2014) 821–823.